

Retinoblastoma Radiotherapy Treatment Optimizations Through GATE Simulations

İbrahim Etem Gül^{1,a}, Sinan Kuday^{2,b,*}

¹ Medical Physics, Health Science Institute, Istanbul Aydın University, 34295, Istanbul, Türkiye

² Department of Physics, Ankara University, Tandogan, 06100, Ankara, Türkiye

*Corresponding author

Research Article

History

Received: 03/08/2022

Accepted: 25/08/2022

Copyright





©2022 Faculty of Science,
Sivas Cumhuriyet University


ABSTRACT


One of the most frequent children tumors in the area around the eyes is defined as retinoblastoma. Proton radiotherapy treatment is a particularly effective type of radiation therapy due to the prolonged survival rates of children with childhood cancers such as retinoblastoma, continued growth of nearby organs and tissues, low radiation dose restriction of vision-related tissues and systems of these tissues. In this study, a geometry phantom including eyeball, lens, lacrimal gland, optic nerve, optic chiasm, retina, cancer, cornea and bone structures was modeled with Monte Carlo simulation tool GATE (vGATE 9.0). With this simulation, the doses absorbed by the tissues were calculated using the DoseActor and TLEDoseActor algorithms. Secondary doses were determined by the TLEDoseActor algorithm. Determination of secondary radiations is important because of the low radiation dose limit of tissues and systems that affect vision. The best treatment results were tried to be obtained by giving the beam thickness of the radiation used in our study, 4 different angles towards the target and different energies. These results show that it can be helpful in calculating a treatment plan for proton therapy in clinical practice.

Keywords: GATE, DoseActor, TLEDoseActor, Proton therapy, Retinoblastoma, Radiotherapy.

 iethemgul@gmail.com

 <https://orcid.org/0000-0001-6972-3635>

 kuday@cern.ch

 <https://orcid.org/0000-0002-0116-5494>

Introduction

Proton therapy affects the proliferation time of cancer cells, disrupts the nutrition of the cells in question, and is an external beam radiotherapy used to break the DNA helix, stop or destroy the proliferation of these unwanted cells. The aim of all external beam treatments is to try to protect the healthy organs from the negative effects of radiation while targeting the unwanted tumor area in the body with radiation therapy [1]. The risk of secondary cancer after traditional radiotherapy, the longer life expectancy in pediatric cancers, the more radiosensitive tissues and organs, while the tissues continue to grow, while the presence of radiation-induced growth disorders makes proton therapy more preferable. Clinical studies on this subject support that proton therapy gives less dose to healthy tissues compared to other radiotherapy techniques [2]. Although proton therapy facilities are quite expensive, the first facilities are built in the USA, Europe and Japan, but the number of facilities has been increasing in China and South Korea in recent years. Significant advances in proton therapy are expected in the next 10 years. Forecasts include: proton therapy systems will continue to shrink in volume, proton dosimetry will become more sophisticated, and devices that change the size and shape of the proton beam, such as multileaf collimators, will allow the treatment of complex tumors, but will also be more effective in very small lesions such as eye tumors. Recent advances have reduced the volumes of proton therapy technology by up to 40

percent. In particular, the development of superconducting magnet technology was influential in the size of the cyclotron that produced the proton beam. In addition, the revolving portal, in the volume of a three storey building, could be significantly reduced. Thus, proton therapy will be considered more cost effective and in the treatment of different types of cancer, and there will be a significant reduction in operating costs. Scientists are working on very finely tuned collimation systems made of different materials to reduce neutron production, which has a high share in secondary radiation. This will be of great importance, especially in patients receiving repeat proton therapy. [3] Proton Interactions Numerous interactions slow down atomic orbital electrons by the Coulomb force. They are deflected from their direction as a result of numerous collisions with the atomic nucleus. Apart from these, in inelastic collisions that occur occasionally with nuclear interactions, the proton collides with one or more protons in the nucleus, releasing the particles, thereby releasing secondary radiations especially neutrons and gamma rays. In particular, the neutron dose is considered unfavorable in proton therapy because of possible long-term effects. Secondary radiations can cause cancer to recur in patients and healthy tissues to receive an extra dose of radiation. [4]

The content of the article is as follows: In the next section, there will be phantom simulation preparation of eye organ geometry, GATE software, algorithms and

calculations used to calculate secondary radiation doses. In the findings section, we conclude our study with the results and interpretation part, which will find the dose values obtained in the cancerous region in the retina and healthy tissues, and the dose distributions out of the area with the GATE software.

Materials and Methods

Geant4 is a program that allows wide use for simulating the penetration of defined particles through matter. Areas of application include studies in high energy, nuclear and accelerator physics, as well as medicine and space sciences. [5]

GATE combines the advantages of reality-tested physics models of the GEANT4 simulation toolset with extensive geometry definition and powerful 3D visualization and original features unique to emission tomography. The program, which consists of several hundred C++ codes, the mechanisms used to manage time, geometry and radioactive resources, creates with C++ codes thanks to GEANT4.

GATE specifically provides modeling capability. It is a program that allows simulating time-dependent physical events such as detector movements or source decay kinetics, time curves based on realistic conditions. [6]

In the Cartesian coordinate system, the Earth volume which we have determined as 5 m, is created in the x, y and z coordinates. Eye globe, Retina, Cornea, Lacrimal gland, Optic nerve, Temporal bone, Nasal bone, Optic chiasm, Lens, and Cancer tissue geometry, element contents were taken from various anatomy books, articles, ICRU Journal, 46, 1992, ICRP 89 data. [7,8,9,10,11,12,13,14]

If we accept the tumor tissue as the center, 800 Thousand Total Number Of Applications protons with the same characteristics of 20 Mev energy and 4 mm

emittance from 4 different points with 45 degree angles target the cancer tissue. By using the Pen Beam Scanning (PBS) method, Secondary Radiation Generation at the beam source is avoided. In treatments with PBS method, Secondary Radiation is caused by nuclear interactions with atoms of cells and tissues within the beam range of the patient. DoseActor and TLDoseActor are deployed to calculate the absorbed doses in all tissues inside and outside the field. DoseActor and TLEDoseActor algorithms will be discussed in the section.

In the simulation, proton beams with 20 MeV energies targeting the cancerous area from 4 different angles were selected and irradiation was carried out with Pen Beam Scanning Method (PBS). Also known as Active Scanning Proton Therapy, PBS uses a magnet system to conduct protons across the entire cross-section and deflect them at the particle exit, thus leading to the development of density modulated proton therapy (IMPT).

IMPT allows use of the entire tumor area to provide a homogeneously dispersed therapy to the target dose. The use of a range deflector in PBS dulls the flank edge, while collimation allows sharpening of the edge with precision from 2 to 4 mm, depending on the depth of the target tumor. The volume defined in the DoseActor is divided into three-dimensional pixels, namely Voxels, and the energies left by the particles passing through the voxels in these three-dimensional boxes are calculated cumulatively, and the total absorbed energy in the tissue is calculated. The TLE trace length estimator quickly calculates the absorbed energies of secondary particles such as photons and neutrons by using the position, velocity and time parameters as in the fog chamber. We put the DoseActor and TLEDoseActors actors which we evaluated in the simulation on all tissues that we defined with codes, and we determined the doses accumulated in these tissues by opening the root file and integrating the cumulative dose values in the graph.

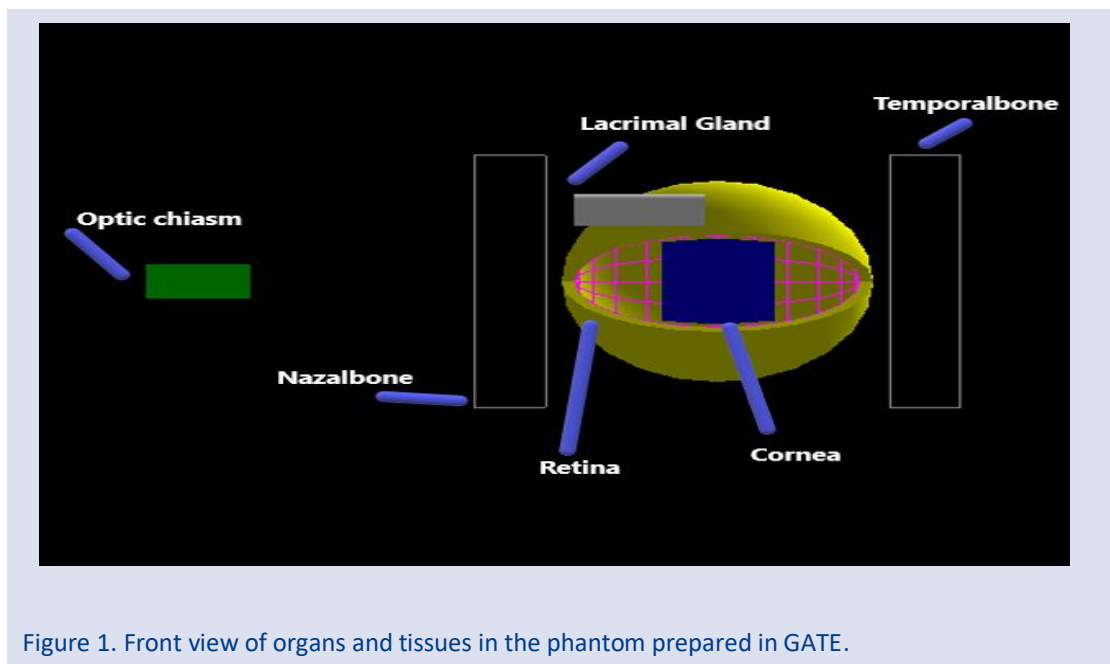


Figure 1. Front view of organs and tissues in the phantom prepared in GATE.

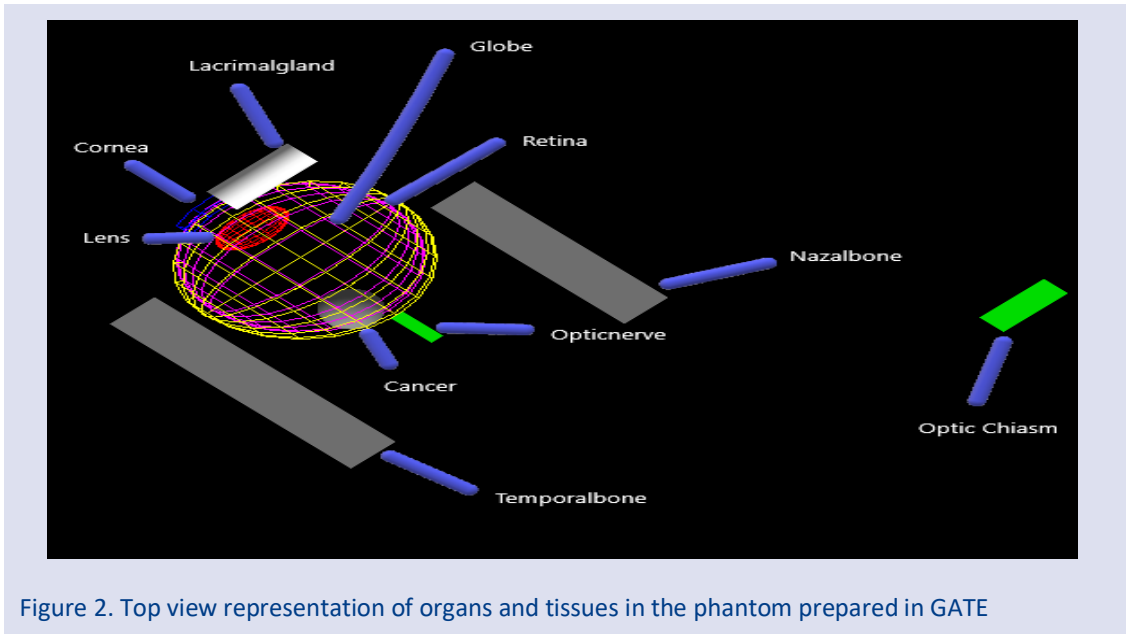


Figure 2. Top view representation of organs and tissues in the phantom prepared in GATE

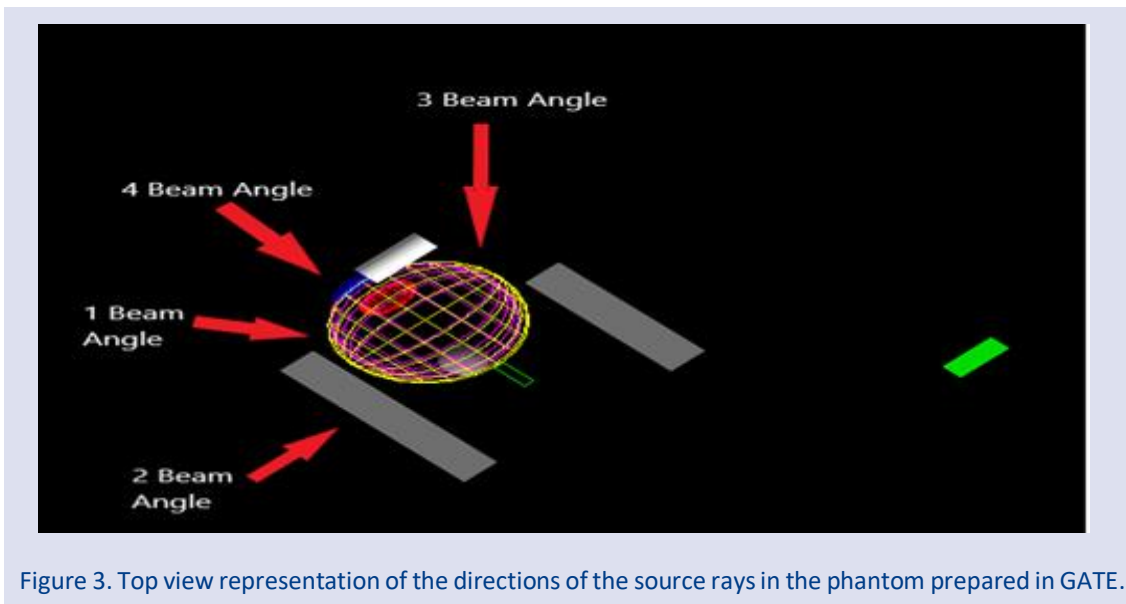


Figure 3. Top view representation of the directions of the source rays in the phantom prepared in GATE.

DoseActor and TLEDoseActor Algorithms

With the GATE 6.2 update made in 2014, DoseActor three-dimensional dose calculation has been enabled. DoseActor can display three-dimensional images and distribution of the energy collected in a certain area. While determining the DoseActor parameters, it is important to choose the voxel sizes according to the needs, the size of the selected volume and the emittance of the beam from the source. It also allows to choose resolution and position. When the DoseActor library is added to the desired volume, it divides it into particles called dosels, and stores all the energies collected in this volume, the uncertainties in the stored energy and dose, the square of the values in the stored energy and dose data, and the values such as the number of interacting particles with the ROOT file. In the volumes we determined in our study, the biochemical composition of

the material was determined beforehand. The DoseActors we place are calculated by dividing the total energy of the material in which it is located by the total volume and density. [17]

The track length estimator (TLE) deterministically calculates the values of secondary radiations (Rayleigh, Compton scattering) occurring after primary interactions using a hybrid algorithm. It calculates the path followed by the particles and the absorbed dose. This calculation is done much faster than conventional methods and can be seen clearly. It is used in MCNPX and MC codes. With the TLE method, it is based on the principle that all voxels in the volumes it encounters throughout the photon range leave their energy behind. For GATE, an algorithm called TLE application EPDL97 is employed. The selected energy range for each element, the coefficients drawn from the table before the simulation starts are loaded and these values are calculated deterministically. [17,18]

Results and Discussion

The secondary radiation values resulting from the interaction of protons with atoms throughout the interval for 10 tissues with different locations and biochemical structures, the cumulative dose values absorbed in the tissues, normalization values and percentage values are given in Table 1 and Table 2. At energies of 15, 20, 25, 30 Mev, a total of 32 different variations are made from 4 different angles with 4mm and 9mm emittance, and different angles are followed. Paired simple t-test was used when calculating statistics. For different values of energy, beam thickness and beam angle, at 5% significance level. The difference was evaluated.

H0: There is no statistically significant difference between 4 mm and 9 mm beam emittance values.

H1: There is a statistically significant difference between the 4 mm and 9 mm beam emittance values. In the second statistical evaluation, different angles were evaluated.

H0: There is no statistically significant difference between the 2nd beam angle and 4th mm beam angle values.

H1: There is a statistically significant difference between the 2nd beam angle and 4th mm beam angle values. In the third statistical analysis, beam energies were evaluated.

H0: There is no statistically significant difference between the values of 15 Mev and 30 Mev.

H1: There is a statistically significant difference between the values of 15 Mev and 30 Mev.

As a result, null hypotheses and alternative hypotheses were established. In the analysis, it was determined that there was a difference in energy values and beam emittance values at the 5% significance level, and there was no difference in the angle values at the same significance level. The confidence interval of the data was calculated. The values we obtained are given in Table 3.

When all energies were analyzed, the optimum values were found to be at 20 Mev energy. It was used at all angles and the advantageous 4mm beam thickness was used. Dose geometries in which tissues were absorbed were determined. 75.44% of the total dose was absorbed

in the tumor. 12.32% of the absorbed dose is absorbed by the Temporalbone, 8.34% by the Globe and 2.84% by the Retina. Dose percentages in non-target tissues remain below 1%. In addition, we could not get dose values in the out-of-range Optic Chiasma, which is very small and very small in volume, and in the Cornea, where we avoided the beam direction. In our study, it was determined that the Proton Emitted Bragg Peak (SOBP) provided high doses to the target volume, while the doses in the organs outside the area were within the dose limit values. Clinically, the treatment of retinalblastoma tumor relies on tumor volume, location, recurrence of cancer primarily in vital organs, and secondarily affecting visual sensation, with a radiation absorption of approximately 1.8 Gy per week traditionally according to the International Classification of Retinoblastoma, issued in 2003 for about 4-5 weeks. It is planned to be treated for only 5 days. At the end of the treatment, it is aimed to give a dose of approximately 45 Gy to the tumor.[1]

In our study, the value exposed to the temporal bone, which is the most dosed healthy structure at a total dose of 45 Gy given for tumor shadow treatment, was calculated as 7.34 Gy. [20] In other sensitive tissues, the dose was well below the limit values. Dose absorption from other tissues was calculated as 4.97 Gy in the eye fluid or globe, 1.69 Gy in the retina, and between 0.01 mGy and 0.53 Gy in other tissues.

In addition to the total absorbed doses in the simulation, the maximum dose was calculated as 1.065 mGy in the cancerous tissue and 0.088 mGy, 0.373 in the lens, retina, optic nerve and optic at the undesired secondary doses and the total doses cooled in the tissues. Chiasmatic tissues which are critical for vision and high radiation sensitivity, respectively. mGy were measured as < 0.001 mGy, < 0.001 mGy. As with Doseactor, no dose value was obtained in the cornea in TLE DoseActor. These values show that proton therapy has a low effect on secondary cancer formation and in tissues with high radiation sensitivity.

Total absorbed doses and percentage values resulting from secondary radiation produced as a result of nuclear interactions during irradiation of retinalblastoma cancer are given in Table 2

Table 1. Dose values cooled in organs and tissues in DoseActor algorithms, percentage values, normalization calculation.

Dose Actor, 800 Thousand Total Number Of Applications, 4 mm Beam Emittance, 20 Mev- 1,2,3,4. Beam Angle			
Organs and Tissue	Total Dose Values	Dosage Value Percentage Values	Normalization Accounts In Gy
Globe	0,064934287	8,34%	4.974 Gy
Cancer	0.58723832	75,43%	45.00Gy
Retina	0.02212048	2,84%	1.694 Gy
Temporalbone	0.095942601	12,32%	7.348 Gy
Nazalbone	1.1824136 e -5	<0.01%	6 mGy
Opticnerve	0.0012386610	0,16%	9,54 mGy
Lacrimalgland	1.0504367 e -5	<0.01%	6 mGy
Lens	0.0069477997	0,89%	0.53 Gy
Opticchiasm	2.7057855 e -8	<0.01%	<0.01 mGY
Cornea			

Table 2. Dose values cooled in organs and tissues in TLEDoseActor algorithms, percentage values, normalization calculation.

TLEDose Actor, 800 Thousand Total Number Of Applications, 4 mm Beam Emittance, 20 Mev- 1,2,3,4. Beam Angle				
Organs and Tissue	Total Dose Values	Dosage Value	Percentage Values	Normalization Accounts In Gy
Globe	1.2168534 e -5	26,29%		0.932 mGy
Cancer	1.3902021 e -5	30,03%		1.065 mGy
Retina	4.8661112 e -6	10,51%		0.373 mGy
Temporalbone	9.7501176 e -6	21,07%		0.747 mGy
Nazalbone	4.3429290 e -6	9,38%		0.332 mGy
Opticnerve	1.555112 e -10	<0.01%		<0.01 mGY
Lacrimalgland	8.2597376 e -8	0,02%		<0.01 mGY
Lens	1.1616141 e -6	2,51%		0.088 mGy
Opticchiasm	8.031298 e -9	<0.01%		<0.01 mGY
Cornea				

Table 3. In the paired sample t test table, the total dose values of all organs include t significance values and confidence intervals.

TLE DOSEACTOR+DOSEACTOR 200 Thousand Total Number Of Applications, 1 Beam Angle , 15 Mev Energy				
Organs and Tissue	4mm Beam Emittance Total Dose Total	9mm Beam Emittance Total Dose Total	D total	D ² total
Total	0,01482031	0,005717856208	9,10238187 . 10 ⁻³	2,039262820042. 10 ⁻⁴
Data	\bar{D}	SD	t account/ t 7,0.05	Confidence Interval
Values	0,001137798	0,0011973757	2,6796 / \pm 2.365	-2,8306 \leq μ D \leq 2,8329
TLE DOSEACTOR+DOSEACTOR 200 Thousand Total Number Of Applications, 4 mm Beam Emittance, 30 Mev Energy				
Organs and Tissue	2. Beam Angle Dose	4. Beam Angle Dose	D total	D ² total
Total	0,01603558534	0,0431035901	9,10238187 . 10 ⁻³	2,039262820042. 10 ⁻⁴
Data	\bar{D}	SD	t account / t 7,0.05	Confidence Interval
Values	-0,00338349591	0,0142164629	-0,6711 / \pm 2.365	-0,0355 \leq μ D \leq 0,02877
TLE DOSEACTOR+DOSEACTOR 200 Thousand Total Number Of Applications, 4 mm Beam Emittance, 2 Beam Angle Dose				
Organs and Tissue	15 Mev Energy	30 Mev Energy	D total	D ² total
Total	0,01777254	0,01665754	0,00175632286405	0,0001716112098014
Data	\bar{D}	SD	t account / t 7,0.05	Confidence Interval
Values	2,1954.10 ⁻⁴	2,1408 .10 ⁻⁵	29,533 / \pm 2.365	1,7.10 ⁻⁴ \leq μ D \leq 2,6.10 ⁻⁴

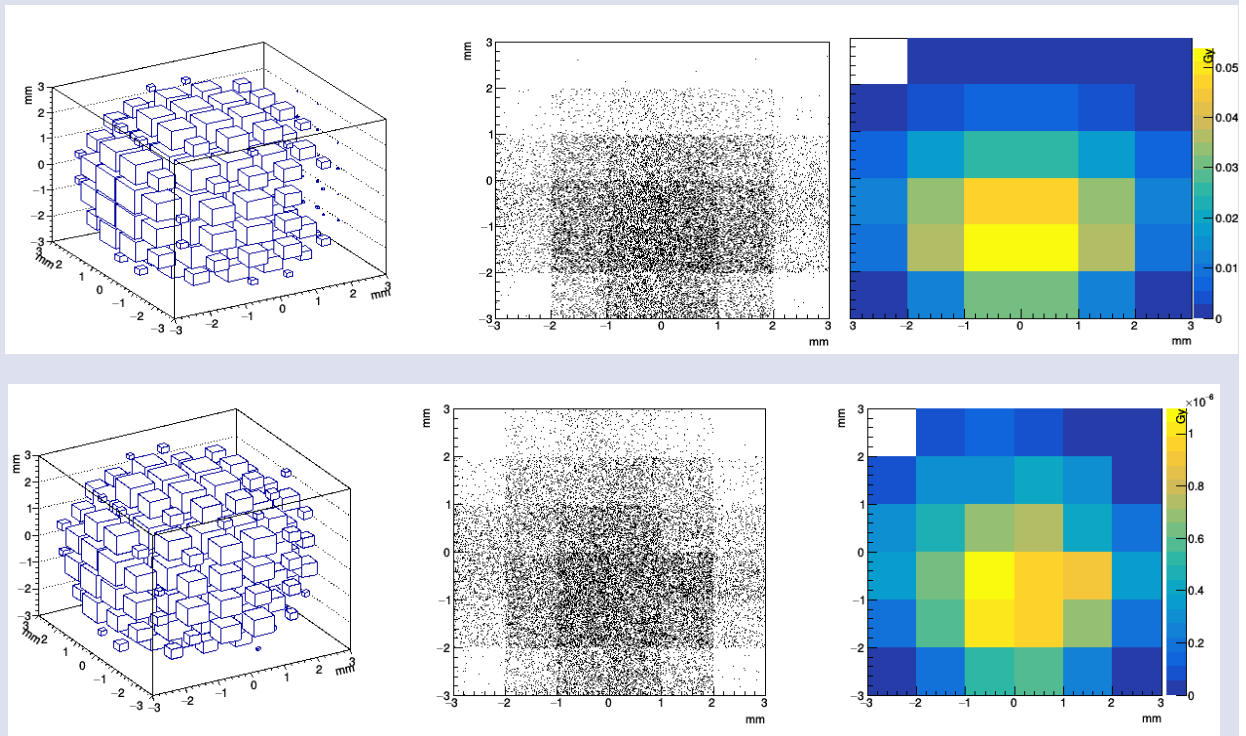


Figure 4. Measured by simulation in cancer tissue; 3B particle distribution (left), 2B particle distribution (centre) dose distribution (right) DoseActor algorithm (top) and TLE algorithm (bottom) dose data.

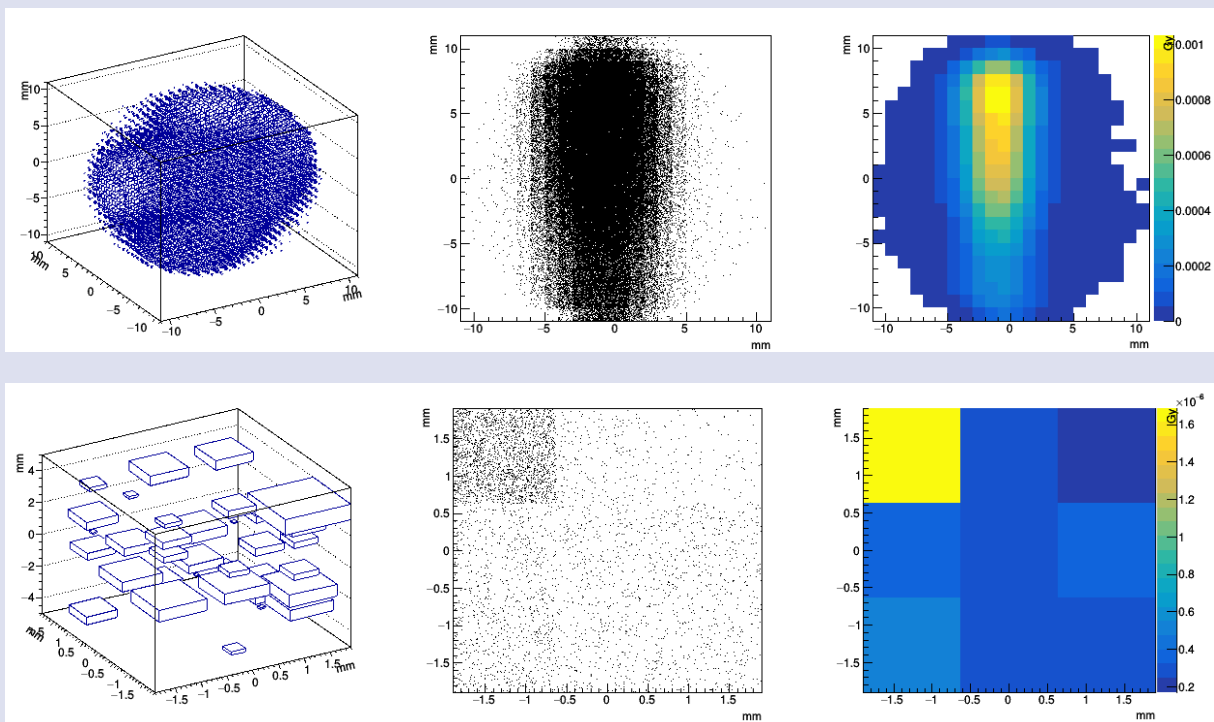


Figure 5. Measured by simulation in globe organ; 3B particle distribution (left), 2B particle distribution (centre) dose distribution (right) DoseActor algorithm (top) and TLE algorithm (bottom) dose data.

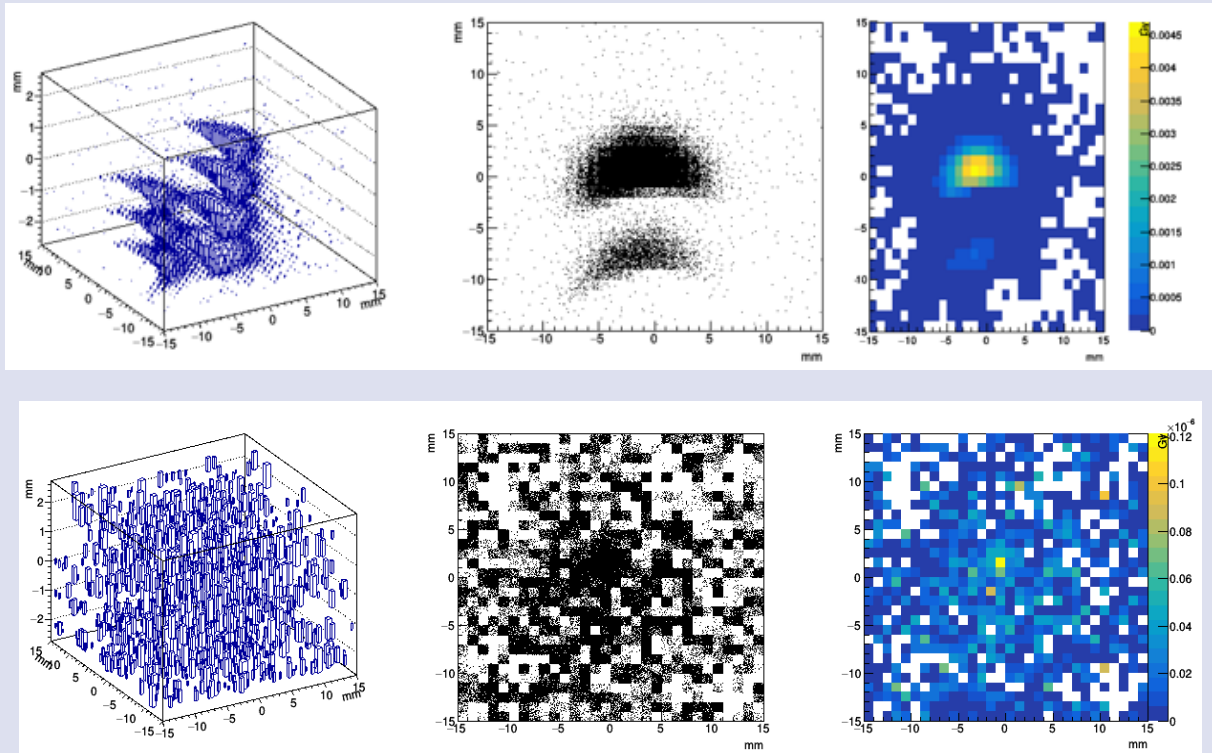


Figure 6. Measured by simulation in temporal bone tissue; 3B particle distribution (left), 2B particle distribution (centre) dose distribution (right) DoseActor algorithm (top) and TLE algorithm (bottom) dose data.

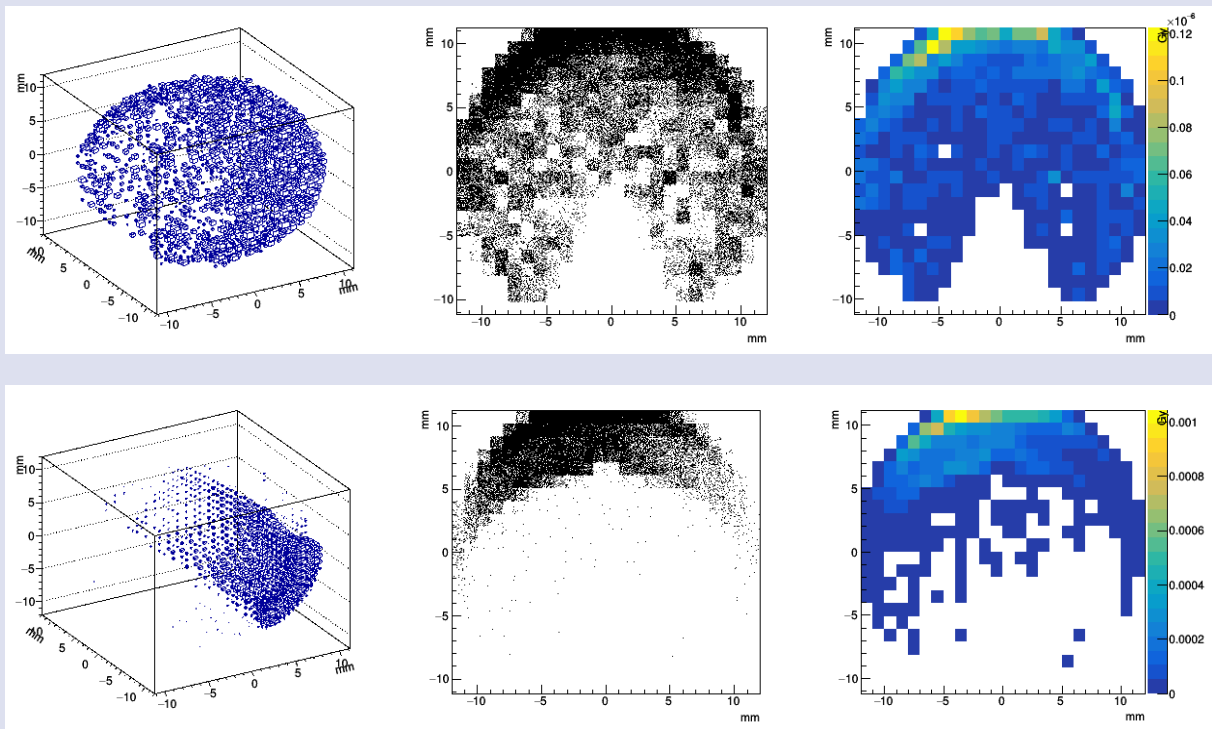


Figure 7. Measured by simulation in cancer tissue; 3B particle distribution (left), 2B particle distribution (centre) dose distribution (right) DoseActor algorithm (top) and TLE algorithm (bottom) dose data.

Conclusion

In our study, we determined the tissue to be given to cancer with a comprehensive trial. When different energy

values, different beam emittance and 4 different angles and paired simple t test values were compared in total dose calculations. A significant difference was found at 5% significance level in beam emittance and different energy

values. When evaluated for radiation given at different angles, no significant difference was observed at the 5% significance level. In the light of these statistics, we experimentally observed that by using different angles to reach the optimum dose. Least damage has been given to different tissues and that there was an improvement as expected. The best target dose was obtained using the beam thickness of 4mm. We also determined that the optimum energy is 20 MeV. It also showed the importance of Geant 4 software for accurate treatment planning because visual sensory tissues are radiosensitive before treatment. It is understood from the data that the effects of secondary radiations originating from unwanted neutrons and photons originating from atomic interactions on tissues are quite limited. At the end of our treatment plan, it was observed that the dose did not accumulate in the tissues above the critical dose value. In addition, the fact that the dose values are seen outside the area shows the importance of using dosimetry in the department employees working with higher energies in the long term.

Conflicts of interest

The authors state that did not have conflict of interests.

References

- [1] Munier F., Verwey J., Pica A., (Eds). New Developments in External Beam Radiotherapy for Retinoblastoma: From Lens To Normal Tissue-Sparing Techniques, *Clinical Experiments Ophthalmology*, 36 (2008) 78-89.
- [2] Lee T., Bilton D., Famiglietti R., (Eds). Treatment Planning With Protons For Pediatric Retinoblastoma, Medulloblastoma, And Pelvic Sarcoma: How Do Protons Compare With Other Conformal Techniques, *International Journal Radiation Oncology Biology Physics*, 36 (2005) 362-372.
- [3] M P Mehta, Proton Therapy Predictions for the Next Decade, Miami Cancer Institute, July 06, 2020.
- [4] Paganetti H. (Eds). Proton Therapy Physics. 1 nd ed. Boston, (2012) 516-544.
- [5] Geant 4 A Simulation Toolkit Available at: https://geant4.web.cern.ch/?statfacts_page=corp. Retrieved August 17, 2022.
- [6] GateOpenGate Collaboration Available at: https://opengate.readthedocs.io/en/latest/introduction/html/?statfacts_page=corp. Retrieved August 17, 2022.
- [7] Başmak H., Gözün Anatomisi ve Fizyolojisi. 1 nd ed. Eskişehir, (2005) 12-44.
- [8] Valentin J.,(Eds). International Commission On Radiological Protection Basic Anatomical and Physiological Data for Use in Radiological Protection Reference Values, *ICRP Publication 89*, 32 (3-4) (2002) 217-220
- [9] Allisy A. (Eds). Reports of the International Commission on Radiation Units and Measurements, *ICRU Publication 46*, 24 (1) (1992) 19-24
- [10] Stafford S., Pollock B., Leavitt J., A Study Of The Radiation Tolerance Of The Optic Nerves And Chiasm After Stereotactic Radiosurgery, *International Journal Radiation Oncology Biology Physics*, 55, (2003) 77-81.
- [11] Vincent Gregoire, Wilfried De Neve, Avraham Eisbruch, Nancy Lee, Danielle Van den Weyngaert, Dirk Van Gestel, Intensity-Modulated Radiation Therapy For Head And Neck Carcinoma, *Oncologist*, 12 (2007) 555-564.
- [12] Haegin Hana, Yeon Soo Yeoma, Thang Tat Nguyen, Chansoo Choia, Hanjin Leea, Bangho Shina, Chan Hyeong Kima, Development of Detailed Eye Models for Pediatric Phantoms, *Transactions of the Korean Nuclear Society Autumn Meeting Gyeongju*, 103 (2017) 6.
- [13] Steven Nguyen, Julian Sison, Marjorie Jones, Jesse L Berry, Jonathan W Kim, A Linn Murphree, Vanessa Salinas, Arthur J Olch, Eric L Chang, Kenneth K Wong, Lens Dose-Response Prediction Modeling and Cataract Incidence in Patients With Retinoblastoma After Lens-Sparing or Whole-Eye Radiation Therapy, *International Journal Radiation Oncology Biology Physics*, 103 (5) (2019) 1143-1150.
- [14] Jones B., Errington D., Proton Beam Radiotherapy, *British Journal Of Radiology*, 73 (2000) 802-805.
- [15] Frances C., Charlwood, A., H., Aitkenhead, Randal I. Mackay, A Monte Carlo Study On The Collimation Of Pencil Beam Scanning Proton Therapy Beams, *Medical Phys.*, 43 (2016) 1462-1472
- [16] Baldacci F., Mittone A., Bravin A., (Eds). A Track Length Estimator Method For Dose Calculations In Low-Energy X-Ray Irradiations, *Implementation, Properties And Performance, Zeitschrift Für Medizinische Physik*, 25 (2015) 36-47.
- [17] Smekens F., Freud N., (Eds). Simulation Of Dose Deposition In Stereotactic Synchrotron Radiation Therapy, *A Fast Approach Combining Monte Carlo And Deterministic Algorithms*, 54 (2009) 4671-4685
- [18] Stewart, F., Akleyev A., Hauer J., (Eds). ICRP Statement on Tissue Reactions and Early and late Effects of Radiation in Normal Tissues and Organs Threshold Doses for Tissue Reactions, *ICRP Publication*, 41 (1-2) (2012) 293-300.